INVERTED MICELLAR INTERMEDIATES AND THE TRANSITIONS BETWEEN LAMELLAR, CUBIC, AND INVERTED HEXAGONAL LIPID PHASES.

II. Implications for Membrane-Membrane Interactions and Membrane Fusion

D. P. SIEGEL
Procter & Gamble Co., P.O. Box 39175, Cincinnati, Ohio 45247

ABSTRACT Results of a kinetic model of thermotropic $L_\alpha \rightarrow H_{II}$ phase transitions (1, 2) are used to predict the types and order-of-magnitude rates of interactions between unilamellar vesicles that can occur by intermediates in the $L_\alpha \rightarrow H_{II}$ phase transition. These interactions are: outer monolayer lipid exchange between vesicles; vesicle leakage subsequent to aggregation; and (only in systems with ratios of L_α and H_{II} phase structural dimensions in a certain range or with unusually large bilayer lateral compressibilities) vesicle fusion with retention of contents. It was previously proposed that inverted micellar structures mediate membrane fusion (e.g., 1, 3, 4). These inverted micellar structures are thought to form in all systems with such transitions (1, 2). However, I show that membrane fusion probably occurs via structures that form from these inverted micellar intermediates, and that fusion should occur in only a sub-set of lipid systems that can adopt the H_{II} phase. For single-component phosphatidylethanolamine (PE) systems with thermotropic $L_\alpha \rightarrow H_{II}$ transitions, lipid exchange should be observed starting at temperatures several degrees below T_H and at all higher temperatures, where T_H is the $L_\alpha \rightarrow H_{II}$ transition temperature. At temperatures above T_H, the H_{II} phase forms between apposed vesicles, and eventually ruptures them (leakage). In most single-component PE systems, fusion via $L_\alpha \rightarrow H_{II}$ transition intermediates should not occur. This is the behavior observed by Bentz, Ellens, Lai, Szoka, et al. (5–8, 9) in PE vesicle systems. Fusion is likely to occur under circumstances in which multilamellar samples of lipid form the so-called "inverted cubic" or "isotropic" phase (19, 20). This is as observed in the mono-methyl DOPE system (Ellens, H., J. Bentz, and F. C. Szoka. 1986. Fusion of phosphatidylethanolamine containing liposomes and the mechanism of the L_α-H_{II} phase transition. *Biochemistry*. In press.) In lipid systems with $L_\alpha \rightarrow H_{II}$ transitions driven by cation binding (e.g., Ca^{2+}-cardiolipin), fusion should be more frequent than in thermotropic systems.

INTRODUCTION

The $L_\alpha \rightarrow H_{II}$ phase transition is an inter-lamellar event: it can only occur when bilayers are closely-apposed (1, 2). Structures that form during this transition should thus allow certain interactions between apposed bilayers. In this paper, I will show what interactions can occur via intermediates in this phase transition in different temperature ranges, and make order-of-magnitude estimates of the rates at which they should occur.

The first intermediates to form in this phase transition are thought (1, 2) to be inverted micellar intermediates (IMI, Fig. 1, top), which form between apposed bilayer membranes. IMI can mediate three types of interactions between lipid vesicles, which are illustrated in Fig. 2. First, IMI make apposed bilayer interfaces momentarily continuous: lipids in the outer monolayers of apposed vesicles can intermix (Fig. 1, top; Fig. 2, top). I will show that IMI can form even when the lipid is at a temperature a few degrees below T_H, the equilibrium $L_\alpha \rightarrow H_{II}$ phase transition temperature.

Second, when the temperature is greater than or equal to T_H, IMI assemble into H_{II} structures (2), converting the facing monolayers of the vesicles into the H_{II} phase. This is an obvious consequence of the existence of the phase transition. It results in rupture and leakage of the vesicles, and more complete lipid mixing (Fig. 2, lower left).

Third, in some but not all systems, it is possible for IMI to form a second type of structure that results in membrane fusion. IMI arte metastable structures in dynamic equilibrium with the original apposed bilayer structure: typical rates of IMI reversion to patches of apposed bilayers are estimated (1, 2) as $\sim 10^3\ s^{-1}$. However, IMI can also revert (1, 2) to another bilayer structure that allows mixing of both the lipids and aqueous contents of apposed vesicles without leakage of the contents to the external medium (interlamellar attachments, or ILA; Fig. 1, bottom; Fig. 2, lower right). This results in membrane fusion. Others (e.g.,

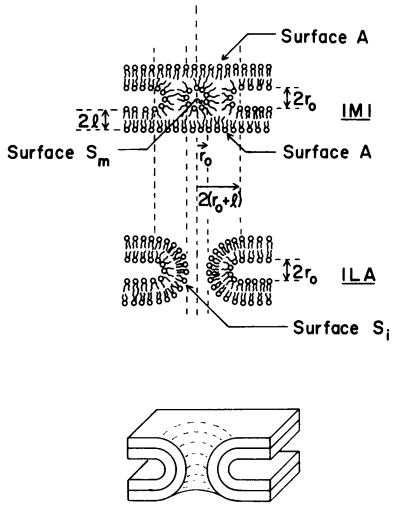

FIGURE 1 IMI (top) and ILA (middle) structures. *Top:* The IMI (1, 2) consists of a spherical inverted micelle (water cavity radius r_0) surrounded by an external monolayer of lipid. The external monolayer is cylindrically symmetrical about the vertical axis of the figure. The smaller radius of curvature of the external monolayers of both the IMI and the ILA (as initially formed) is r_0. Surfaces A are the circular areas of planar monolayer (radius = $2[r_0 + l]$) above and below the high-curvature surfaces of the IMI. Surface S_m is the lipid-water interface inside the spherical micelle. *Middle:* The ILA is also cylindrically symmetrical about the vertical axis, and makes the two original bilayers continuous around the edge of an interlamellar pore. S_i is the surface lining this pore. *Bottom:* Cross-section of ILA, viewed in perspective.

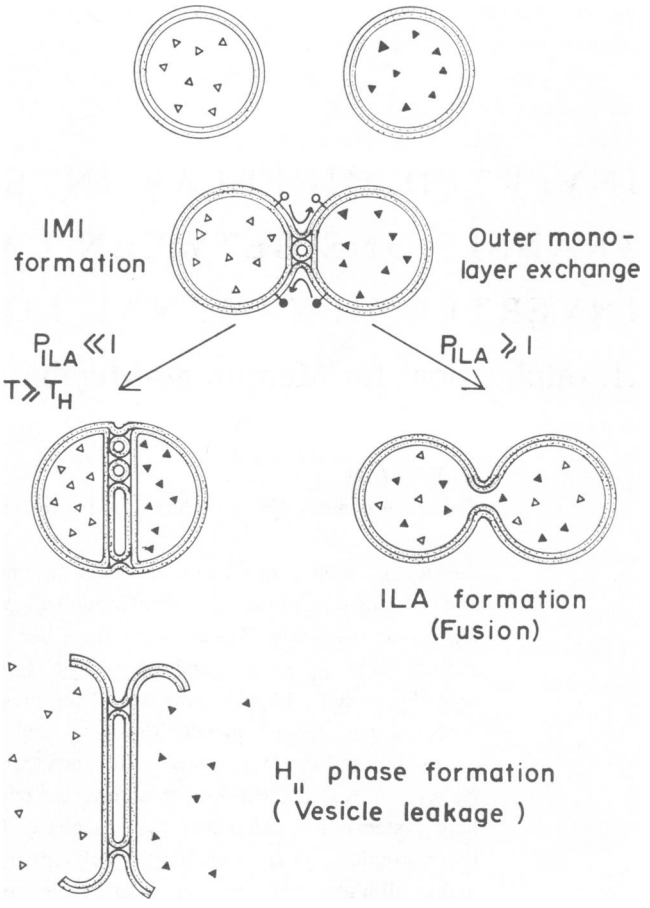

FIGURE 2 Membrane-membrane interactions that can occur via IMI in lipid vesicle dispersions. When IMI form between two vesicles, the outer monolayers of the membranes become continuous, allowing lipid molecules to diffuse back and forth between the two vesicles. When P_{ILA} is $\gtrsim 1$, ILA form fast enough to appear before all IMI are consumed via H_{II} phase formation. This results (*right* side of figure) in mixing of the aqueous contents of the two vesicles without leakage to the external medium (fusion). Fusion can occur when T is greater than or equal to T_H, but may be possible a couple of degrees below T_H in some cases. If P_{ILA} is $\ll 1$, and T is $\geq T_H$, then the H_{II} phase forms between the apposed vesicles (*left* side of figure). This eventually ruptures the vesicles, releasing the aqueous contents to the external medium (*bottom*).

3, 4) have previously proposed a role for IMI (which correspond to the "lipidic particles" they discuss; 1) in membrane fusion. However, whereas IMI are probably involved in all $L_\alpha \rightarrow H_{II}$ transitions (2), I will show that ILA can form in only a sub-set of systems with this phase transition. Hence, fusion via $L_\alpha \rightarrow H_{II}$ transition intermediates will be observed only in those systems.

These predictions are consistent with observed membrane-membrane interactions in H_{II}-forming systems (5–10). The kinetic description developed here is applicable to lipids undergoing thermotropic $L_\alpha \rightarrow H_{II}$ phase transitions, and is only a qualitative guide to the behavior of systems in which the transition is driven by cation-binding (e.g., Ca^{2+}-cardiolipin; 11, 12).

THEORY

Overview

IMI are probably the first structures to form during the $L_\alpha \rightarrow H_{II}$ phase transition, making the facing monolayers of apposed bilayers continuous (1, 2). IMI form in large numbers when membranes are apposed near T_H (10^{10} to 10^{11} per cm^2 of bilayer interface in systems near the phase transition; e.g., 13). It is easy to show (Eq. 26, below) that the expected order-of-magnitude lifetime of an IMI (10^{-3} s; 1, 2) is large compared with the random-walk diffusion time of a lipid molecule across the surface of a vesicle 0.1 μm or more in diameter: a single IMI can rapidly mix the outer monolayers of apposed vesicles. IMI ("lipidic particles") are observed in freeze-fracture electron micrographs of L_α phase samples near this phase transition (e.g., 13). Near T_H, the number of observable IMI decreases as the L_α phase is stabilized either by reduction in temperature or by addition of increasing mole fractions of a lipid that only adopts the L_α phase (1, 13). We thus expect that IMI may begin forming between apposed vesicles at temperatures slightly lower than T_H and at all higher temperatures. Estimates of IMI formation rates (1, 2) show that this should happen within a second or less after vesicle aggregation.

When the temperature is greater than T_H, IMI formed between the two vesicles aggregate into H_{II} precursors (2). More and more vesicle surface will be apposed to convert

as much lipid as possible to the H_{II} phase, and a tension will develop in the vesicle walls that eventually becomes sufficient to rupture them. This produces vesicle leakage and more extensive lipid mixing than isolated IMI formation (sheets of membrane from ruptured vesicles can join edge-on, producing complete lipid mixing). Since leakage is driven by the $L_\alpha \rightarrow H_{II}$ transition in apposed bilayer areas, such leakage will occur within a time after vesicle aggregation roughly equal to the $L_\alpha \rightarrow H_{II}$ phase transition time. This time is estimated from theory to be on the order of 10^{-1} to -1 s for unsaturated acyl-chain phosphatidylethanolamines (PEs) superheated by 1° K (2), and is observed to be ~1 s or less for PEs subjected to large temperature jumps (14, 15; P. Laggner, personal communication). Thus, lipid exchange and vesicle leakage should be complete within seconds or less after vesicle aggregation.

IMI are in dynamic equilibrium with the bilayers from which they form, and can revert to patches of planar bilayer on a millisecond time scale (1, 2). The extent to which fusion occurs is determined by the rate at which IMI revert instead of another type of bilayer structure, the inter-lamellar attachment (2), or ILA (Fig. 1, bottom).

More specifically, fusion will occur via ILA only if the rate of ILA production is comparable to or greater than the rate at which IMI are consumed by H_{II} phase formation. During the phase transition, the steady-state number of IMI per unit area of apposed bilayer-bilayer interface is termed n_I^0 (2). n_I^0 is estimated (2) and observed ("lipidic particles"; e.g., 13) to be on the order of 10^{10} to 10^{11} structures per centimeter squared. These IMI are consumed via coalescence into H_{II} precursors at a rate $k_I(n_I^0)^2$, where k_I is a rate constant $\approx 10^{-11}$ cm^2/s (2). Let P_{ILA} be the rate at which an ILA can form from an IMI. The two rates at which IMI are consumed are:

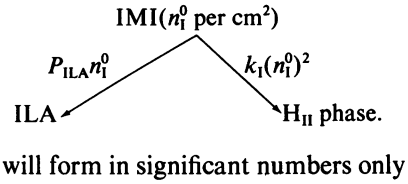

ILA will form in significant numbers only if

$$P_{ILA} \gtrsim k_I n_I^0 \approx 10^{-1}\text{–}1\ \text{s}^{-1}. \quad (1)$$

I will show first that ILA form rarely in most systems (i.e., $P_{ILA} \ll 1$) because a major lipid concentration fluctuation must occur in an IMI in order for it to rearrange into an ILA. The frequency of such fluctuations decreases precipitiously with increasing size of the required fluctuation (1). In contrast, no fluctuation is necessary for IMI reversion to planar bilayers (1). Hence, few if any ILA are produced from IMI unless only a very small concentration fluctuation is required.

The frequency of the required concentration fluctuation is very sensitive to the ratio of the areas per lipid molecule head group in the L_α and H_{II} phase ($\bar{a}$ and a_0, respectively). I will show that ILA formation (and hence fusion) is much more probable (by orders of magnitude) in systems with smaller values of this ratio than are found in pure phosphatidylethanolamine systems. More specifically, I estimate that if this ratio is much greater than roughly 1.2, P_{ILA} will be very small compared to unity, and an ILA will not be able to form between two vesicles and fuse them before all the IMI are converted to the H_{II} phase (Eq. 1). This ratio is more than 1.2 for most single-component H_{II}-forming lipids. It is ~1.8 for egg phosphatidylethanolamine (16, 17), which should be typical of most unsaturated acyl-chain phosphatidylethanolamines (PE). Fusion via ILA should be rare in such systems, and fusion is not observed in pure PE systems (9). The frequency of the fluctuation required for ILA formation is also very sensitive to the lateral compressibility of the bilayers (1), large compressibilities corresponding to large formation rates.

The head group area ratio is related to the equilibrium curvature of the H_{II} phase in a given lipid system. Smaller H_{II} tube diameters correspond to greater differences in a_0 and $\bar{a}$. Lipids with larger head groups are likely to have larger a_0 and smaller $\bar{a}/a_0$ ratios, since it is harder to pack large head groups close together in the H_{II} phase than in the L_α phase. Thus, the ratio is likely to be small in mixtures of PE with phosphatidylcholines (PCs), since in these system the H_{II} tube diameter increases rapidly with increasing PC content (20), while $\bar{a}$ in the L_α phase is nearly the same for many unsaturated acyl-chain PEs and PCs (17). The ratio is also likely to be small in single-component systems with slightly larger head groups than PE (e.g., mono-methylated PE; 17). Morphology consistent with ILA is observed in such cases (particularly systems incorporating some cholesterol; e.g., Figs. 5 and 6, and other systems reviewed in reference 19). Elsewhere (D. P. Siegel, manuscript submitted for publication) I will show that ILA in multilamellar arrays should assemble into a structure resembling the inverted cubic phase described by others (18, 20, 21), and that such "phases" are more probably metastable arrays of these intermediates. These "phases" should be observed in systems with $P_{ILA} \approx 10^{-1}$–1 (Eq. 1). Unilamellar vesicles should fuse via ILA formation under the same conditions in which multilamellar samples of the same lipids form cubic or isotropic phases.

The rates of ILA formation estimated here are only order-of-magnitude estimates because the dimensions of the transient intermediates are not susceptible to direct measurement and the lateral compressibilities haven't been measured in relevant systems. However, the results are accurate enough to verify that ILA shouldn't form in pure PE systems, where they are not observed, and *are* likely to form in PC-PE mixtures and in mono-methylated PE, where morphology consistent with them and the so-called "cubic phases" are observed.

In systems where ILA form fairly rapidly at $T \gtrsim T_H$, whatever fusion that occurs must also be complete within

an interval equal to the phase transition time after vesicle aggregation. The proportion of vesicle-vesicle contacts that result in fusion, however, may have an odd temperature dependence. This proportion is determined by the probability that an ILA forms before the lipid of the apposed interfaces is converted to the H_{II} phase. The fusion rate via ILA may be maximal a couple of degrees below T_H, since in this temperature range, a few IMI can form and revert as long as the vesicles remain aggregated, but IMI are not consumed by H_{II} phase formation. In contrast, at $T \geq T_H$ IMI are more rapidly consumed via H_{II} formation (Eq. 1) and are not able to form ILA.

First I will derive estimates of the formation rate of ILA from IMI. Then I will use the theory in (1, 2) to verify that the IMI formation rate between apposed vesicles is rapid, verify that IMI can extensively mix outer monolayers of apposed vesicles, derive conditions for vesicle leakage via H_{II} phase formation, and crudely estimate a temperature dependence of the IMI formation rate near T_H.

Rate of IMI Reversion to Interlamellar Attachments (ILA)

P_{ILA}, the ILA Formation Rate. When an IMI forms an ILA, the dimensions of the exterior monolayer of the ILA should be the same as those of the IMI. The radius of the water cavity in the inverted micelle and the smaller principle radius of curvature of the exterior surface of an IMI are both about the value r_0 given by Eq. 64 of reference 1;

$$r_0 = \frac{-B + [B^2 - 8Wl^2]^{1/2}}{2W} \tag{2}$$

$$B = l(4 - \pi b);\ W = 2 - b(\pi + b - 1);\ b = (\bar{a}/a_0)^{1/2}$$

l is the monolayer thickness, $\bar{a}$ is the area per lipid head group in the L_α phase, and a_0 the area per head group in the H_{II} phase. r_0 is also the radius of the narrowest part of the channel through the ILA (Fig. 1). During ILA formation, patches of monolayer above and below the inverted micelle in the IMI (surfaces A, Fig. 1) and the lipid of the inverted micelle (surface S_m, Fig. 1) rearrange into a monolayer lining the channel through the ILA (surface S_i).

Because the areas of these surfaces are different and the areas per lipid molecule on them are not all the same (1), the number of lipid molecules in monolayer S_i is often larger than the number in the monolayers of the original IMI. Let the number of lipid molecules in the monolayer area S_i, A, and S_m be n_i, n_l, and n_m, respectively. In order for an ILA to form, $n_i - n_m$ molecules must be present in the two monolayers A, which are each composed of n_l molecules at equilibrium. The required increment in the number of molecules on the surfaces A *is* $\Delta n = n_i - n_m - 2n_l$. The time scale for IMI reversion is in the 10–100 ns range (1, 2), which is fast compared with the random-walk diffusion time of lipid molecules across the dimensions of an IMI ($\sim 1\ \mu s$). Therefore, the increment Δn must be about evenly-divided between the two surfaces A or an ILA will not be able to form: there must be a simultaneous concentration fluctuation (increment of $\Delta n/2$ molecules) in each surface. Otherwise, the lipid molecules could not rearrange into the ILA structure on the time scale of ILA formation. The relative magnitude of the required fluctuation is

$$\tilde{n}_c = \frac{\Delta n}{2n_l} - 1 = \frac{(n_i - n_m)}{2n_l} - 1. \tag{3}$$

As described in reference 1, the probability of a fluctuation of this magnitude occurring simultaneously in both surfaces A is

$$P_f = (1/4)\left[erfc\left\{\tilde{n}_c\left(\frac{A}{2kTC_s}\right)^{1/2}\right\}\right]^2, \tag{4}$$

where C_s is the lateral compressibility of the bilayer. The rate at which these fluctuations occur in an IMI is the product of P_f and the frequency of concentration fluctuations, f. f is the inverse of the two-dimensional random-walk diffusion time of a lipid molecule across a monolayer patch of area A,

$$f = 4\pi D/A, \tag{5}$$

where D is the diffusion coefficient of the lipid molecules within the bilayer and $A = 4\pi(r_0 + 1)^2$. The probability (≤ 1) that an ILA will form from the IMI undergoing these critical fluctuations (Eq. 16 of reference 1), is F

$$F = \frac{\alpha_1 A}{4\pi D}\exp\left\{-\frac{G_{ILA}}{kT}\right\} \qquad (F \leq 1), \tag{6}$$

where G_{ILA} is the activation energy for ILA formation (discussed below). α_1 is the lipid molecule lateral displacement rate in the bilayers, which is $\sim 10^8\ s^{-1}$. Thus, the rate of ILA formation from an IMI is

$$P_{ILA} = \frac{\pi D}{A}\left[erfc\left\{\tilde{n}_c\left(\frac{A}{2kTC_s}\right)^{1/2}\right\}\right]^2 F. \tag{7}$$

The magnitude of P_{ILA} is determined chiefly by the magnitude of $\tilde{n}_c$, to which it is extremely sensitive through the $[erfc\ (x)]^2$ term. $[erfc(x)]^2$ is a precipitously decreasing function of its argument, having the values 2×10^{-5}, 5×10^{-10}, and 2×10^{-16} for $x = 2$, 3, and 4, respectively. It will be shown below that to a good approximation, F is unity for relevant values of $\tilde{n}_c$.

Magnitude of $\tilde{n}_c$. To calculate $\tilde{n}_c$ (Eq. 3), we need to know n_i, the number on molecules on surface S_i. n_i is S_i divided by the average area/lipid molecule on S_i. The arrangement of lipid molecules on S_i ranges between packings almost identical with the H_{II} and L_α phases. Where S_i becomes continuous with the monolayers of the apposed bilayers, the area per head group must be $\bar{a}$, as in

the L_α phase. At the narrowest portion ("neck") of the channel through the ILA, the channel radius (r_0, Eq. 2) is about the radius of the water channel in the H_{II} phase, so that the area per head group must be about a_0. We don't know the dependence of the area per head group on the local interfacial curvature for intermediate values. It seems reasonable to assume that the area per head group will be a_0 in the "neck" over a band of height $2r_0$ (i.e., extending a distance r_0 to either side of a plane equidistant between the two apposed bilayers). For simplicity, I assume that the head group area is $\bar{a}$ everywhere else. (Below, I will show how the predicted value of $\tilde{n}_c$ changes when the other possible assumptions about this dependence are made.) The number of molecules on S_i is then

$$n_i = \frac{(S_i - 4\pi r_0^2)}{\bar{a}} + \frac{4\pi r_0^2}{a_0}. \tag{8}$$

n_m (1, 2) and n_l in Eq. 3 are given by

$$n_m = \frac{S_m}{a_0} = \frac{4\pi r_0^2}{a_0},$$

$$n_l = \frac{A}{\bar{a}} = \frac{4\pi(r_0 + l)^2}{\bar{a}}. \tag{9}$$

S_i is

$$S_i = 4\pi^2(r_0 + l)(r_0 + 2l) - 4\pi(r_0 + 2l)^2. \tag{10}$$

With Eqs. 3 and 9, we find

$$\tilde{n}_c = \frac{S_i - S_m}{2A} - 1. \tag{11}$$

This expression can be written in terms of the ratio r_0/l;

$$\tilde{n}_c = \frac{\pi\left[1 + \frac{l}{r_0 + l}\right] - \left[1 + \frac{l}{r_0 + l}\right]^2 - \left[\frac{r_0}{r_0 + l}\right]^2}{2} - 1. \tag{12}$$

By substituting for r_0 (Eq. 2), $\tilde{n}_c$ is obtained in terms of $\bar{a}/a_0$ · $\tilde{n}_c$ is plotted as a function of (r_0/l) and $(\bar{a}/a_0)$ in Fig. 3. $\bar{a}$ and a_0 are structural parameters of the equilibrium phases, which are determined via x-ray diffraction.

The ratio $\bar{a}/a_0$ reflects the equilibrium interfacial curvature of the lipid system. (This factor is similar to the intrinsic curvature discussed in reference 29). Systems in which the equilibrium curvature is small (small a_0, thus small r_0 and large $\bar{a}/a_0$) will not form ILA because $\tilde{n}_c$ will be too large and thus P_{ILA} will be nearly zero (Eq. 7). We can thus estimate the rate of ILA formation per IMI on the basis of $\bar{a}$ and a_0. For typical D, A, α_l, and C_s (7×10^{-8} cm^2/s (22, 23), 10^{-12} cm^2, 10^8 s^{-1}, 10^{-2} cm/dyne (24), respectively) and $F = 1$, the maximum ILA formation rate (Eq. 7) is on the order of

$$P_{ILA} \approx 10^5[erfc\{35\tilde{n}_c\}]^2 \text{ per IMI per second.} \tag{13}$$

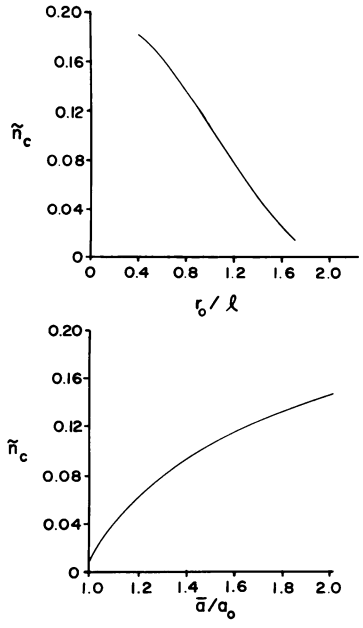

FIGURE 3 *Top:* Scaled magnitude of the critical lipid concentration fluctuation in Surfaces A necessary for ILA formation, $\tilde{n}_c$, vs. r_0/l. *Bottom:* $\tilde{n}_c$ vs. $\bar{a}/a_0$. P_{ILA} becomes significant compared to unity only if $\tilde{n}_c \leq 0.06$.

With Fig. 3 and Eq. 13, we can estimate the value of $\bar{a}/a_0$ for which P_{ILA} approaches 1 s^{-1} and membrane fusion via ILA becomes possible. $[erfc(2)]^2$ is 2×10^{-5}, so that P_{ILA} should approach this rate when $\tilde{n}_c$ is $\leq 2/35$, or $\tilde{n}_c < 0.06$. Fig. 3 shows that this is true for systems in which $\bar{a}/a_0 \lesssim 1.2$.

P_{ILA} for unsaturated acyl-chain PE systems can be estimated as follows. The value of $\bar{a}/a_0$ for egg PE ≈ 1.8 (using $\bar{a}$ and a_0 from references 16, 17). With $r_0 = 1.34$ nm (Eq. 1) and $l = 1.6$ nm (egg PE; 17), $\tilde{n}_c = 0.130$ (Eq. 12). The bilayer compressibility, C_s, as measured directly via dilation of single egg- and dimyristoyl-PC bilayers (24, 25), is 0.007 cm/dyn. The value for PE may be somewhat different. We use a value of $C_s \approx 0.01$ cm/dyne, which is the value calculated (1) from the data for mixtures of saturated and unsaturated PEs in reference 26. (The larger values of C_s used in reference 1 are now thought to be inaccurate; 27, 28). We use $D = 7 \times 10^{-8}$ cm^2/s, and A is calculated with Eq. 9. We use the upper limit on F of unity to find the upper limit on P_{ILA} (Eq. 7);

$$\text{PE systems: } P_{ILA} \approx 10^5[erfc(4.8)]^2F \approx 10^{-17} \text{ ILA/s.}$$

Obviously, this formation rate is negligable (Eq. 1), and we do not expect to observe ILA formation in such systems.

This estimate of P_{ILA} is very sensitive to $\tilde{n}_c$. As calculated here, $\tilde{n}_c$ is approximate, and therefore so is the critical value of $\bar{a}/a_0$ for which ILA formation becomes rapid. The uncertainty results from having to assume values for the area/lipid molecule on surface S_i. However, we can put limits on the range of $\tilde{n}_c$ for a system with a given value of $\bar{a}/a_0$. Let the average area per molecule on S_i be β. It can

be shown that

$$\tilde{n}_c = \frac{\pi\left[1 + \frac{l}{r_0 + l}\right] - \left[1 + \frac{l}{r_0 + l}\right]^2 - \left[\frac{r_0}{r_0 + l}\right]^2\left[\frac{\beta}{a_0}\right]}{(2\beta/\bar{a})} - 1. \quad (14)$$

The area of the region where the area/lipid has to be about a_0 is approximately $4\pi r_0^2/S_i$, or roughly 10% S_i for $r_0 \approx 1$. $\bar{a}/a_0$ is almost certainly <2. I know of no system with such a large ratio, and it is usually smaller, e.g., in egg PE. Thus it is unlikely that β is less than $\bar{a}/[0.9 + 0.1(2)]$ or $0.91\bar{a}$. Conversely, β is unlikely to be greater than $\bar{a}$ for two reasons. First, as just discussed there is a substantial part of S_i with the smaller area/lipid of a_0. Second, Eqs. 17–19, below, show that the net area-average curvature of S_i is negative (head groups packed slightly closer together than on planar interfaces; i.e., $\beta < \bar{a}$) throughout the relevant range of r_0 and l ($0 < r_0 \lesssim 3.5\, l$). For egg PE, the lower and upper limits on β yield $\tilde{n}_c$ values of 0.17 and 0.05, respectively. The former value produces a P_{ILA} that is essentially zero, consistent with the trivial value of P_{ILA} given by Eq. 12. The latter value yields an upper limit on P_{ILA} of $\sim 10^1$ ILA s^{-1}. This rate is larger than our estimate of the rate of IMI assembly into the H_{II} phase (Eq. 1), but the value of β that yields this limit is very unlikely.

Therefore, these order-of-magnitude estimates show that ILA probably do not form at observable rates in unsaturated acyl-chain PE systems across the possible range of $\tilde{n}_c$ values. Even with the unlikely assumption $\beta = \bar{a}$, Eqs. 12 and 14 both show that the rate of formation of ILA is many orders of magnitude faster in systems with small values of the ratio $\bar{a}/a_0$ than in systems with the $\bar{a}/a_0$ values found in systems like egg PE. This is in accord with the fact that morphology consistent with ILA has not been reported in pure PE systems. Morphology consistent with ILA and the inverted cubic phase that is thought to form from them (D. P. Siegel, manuscript submitted for publication) has only been observed in systems with smaller $\bar{a}/a_o$, such as PE to which small mole fractions of L_α phase PC has been added (19, 20, 21).

Activation Energy for ILA Formation. The activation energy for ILA formation, G_{ILA}, determines the value of F. However, G_{ILA} is also determined by $\tilde{n}_c$. I will now show that the dependence of G_{ILA} on $\tilde{n}_c$ is such that F is simply equal to one for $\tilde{n}_c$ much greater than zero. This greatly simplifies our estimates of P_{ILA} (Eq. 7). We don't need accurate estimates of G_{ILA} to demonstrate this. G_{ILA} is composed of three contributions

$$G_{ILA} = G^{\ddagger}_{-} + G_s - G_f. \quad (15)$$

$G^{\ddagger}_{-}$ is the activation energy for the information of two lipid-water interfaces from interface S_m, and is the same as for IMI reversion of planar bilayers (1, 2): it was estimated in references 1 and 2 to be $\sim 10\, kT$ for PE systems. G_s is the free energy necessary to form the surface S_i with its nonequilibrium radii of curvature (analogous to G_{def} in references 1 and 2). G_f is analogous to G_c of reference 1. G_f is the increase in free energy of the lipid in surface A (decrease in activation energy) due to the critical fluctuation. G_f is given by (1)

$$G_f = 2(1 + \tilde{n}_c)n_l\left[\left(\frac{\bar{a}}{C_s}\right)\left\{\frac{1}{1 + \tilde{n}_c} - 1\right\}^2\right]. \quad (16)$$

G_f is a rapidly increasing function of $\tilde{n}_c$, and can be tens of kT (1). It is of most interest to us here because it demonstrates the effect of $\tilde{n}_c$.

The curvature free energy G_s of ILA can be estimated as was the IMI curvature free energy G_{def} in reference 2. Let k_e be the bending modulus of the lipid-water interfaces. We use the same assumptions about the equilibrium curvature in the two regions of S_i as we did in deriving Eq. 11. It can be shown that for r_0 smaller than $3l$, the curvature free energy of surface S_i (excluding the band in the neck with H_{II}-like curvature) is to a good approximation given by

$$G_s = S_i k_e\left[-\frac{1}{R'} + \frac{1}{r_0 + 2l} - \frac{1}{R_0}\right]^2, \quad (17)$$

where

$$\frac{1}{R'} = \frac{2\pi^2(r_0 + 2l) - 4\pi r_0^2}{S_i} \quad (18)$$

and

$$S_i \approx 4\pi^2(r_0 + l)(r_0 + 2l) - 4\pi(r_0 + 2l)^2. \quad (19)$$

R_0 is the equilibrium radius of curvature for the interface. R_0 is infinity in the L_α phase, which is appropriate for this portion of S_i. Expressions like Eqs. 17 and 18 can be derived for the H_{II}-like region of S_i, but the net curvature in this region is so close to the equilibrium curvature of the H_{II} phase that the contribution to the total curvature energy is often less than kT. k_e must be on the same order of magnitude as the values for bilayers (10^{-12} erg; 29–32). With $k_e \approx 10^{-12}$ erg, r_0 and l determined for egg PE as before, we obtain $G_s \approx 20\, kT$.

The important points are: first; that the sum of $G^{\ddagger}_{-}$ and G_s in Eq. 15 is likely to be 30-40 kT; and second; that G_f (Eq. 16) will approach this value when $\tilde{n}_c \gtrsim 0.07$. The total G_{ILA} will be close to zero under these conditions, and F will have the maximum value of unity (Eq. 6). We can thus assume that $F = 1$ for most values of $\bar{a}/a_0$, which greatly simplifies our estimates of P_{ILA}. However, note that G_{ILA} will increase and F will decrease for smaller values of $\tilde{n}_c$, which will therefore decrease P_{ILA} (Eq. 7). This decrease in F for values of $\tilde{n}_c$ smaller than $\tilde{n}_c \approx 0.07$ may indicate that ILA can form only when $\tilde{n}_c$ is in a narrow range around 0.07. However, our estimates of $\tilde{n}_c$ and activation energies are too crude to make more refined predictions concerning this point.

Probability of Vesicle-Vesicle Fusion via ILA. Two aggregated vesicles fuse when at least one ILA forms between them before they leak or disaggregate. Let P_f be the number of ILA that can form between two vesicles apposed over an area of contact A_c before the lipid in this region enters the H_{II} phase. The number of ILA forming per unit time is

$$A_c n_I^0 P_{ILA}. \tag{20}$$

n_I^0 is estimated to be 10^{10} to 10^{11} cm^{-2} (2). The total number of ILA we can expect to form between two vesicles is approximately

$$P_f \approx A_c P_{ILA} n_I^0 t_T. \tag{21}$$

t_T is the length of time required to transform the lipid on the exterior of the vesicles in area A_c into the H_{II} phase. This time will be about the bulk phase transition time t_T estimated (2) and observed (14, 15; P. Laggner, personal communication) to be ~1 s or less.

The rate of ILA-mediated fusion is dictated primarily by the magnitude of P_{ILA}. For vesicles 0.1 μm in diameter, A_c will be ~10^{-11} cm^2 (i.e., a circular patch of membrane ~30 nm in diameter), so that

$$P_f \approx (10^{-1}\text{–}1) \cdot P_{ILA}. \tag{22}$$

The apparent first-order rate constant for fusion of two apposed vesicles in an aggregate is

$$k_f = \frac{P_f}{t_T}. \tag{23}$$

P_{ILA} must be significant compared to unity in order for k_f to approach the range of k_f measured (33, 34) for non-H_{II}-forming, non-ILA-forming systems (35–37). Note that the expression for k_f in Eq. 23 is different from the form in (1), where it was assumed that P_{ILA} was 0.5 in all cases. In view of the calculations of P_{ILA} in this paper, this is clearly incorrect.

Leakage of Aggregated Vesicles Induced By H_{II} Phase Formation

Leakage will be observed before fusion in systems for which P_f is small compared to unity and T is greater than T_H. As the lipid in A_c enters the H_{II} phase, a tension is induced in the vesicle walls. The surfaces of the membranes must be apposed in order to form the H_{II} phase, but the surface area of the vesicles is essentially constant. The vesicles deform as the area of the diaphragm between them increases. Eventually, either the tension in the vesicle walls prevents further growth of the H_{II} phase region or the walls rupture and the vesicles leak. In order to rupture the vesicles, the free energy reduction achieved by a virtual expansion of the contact area must exceed the work done against the tension in the membranes when the tension has reached τ^*, the critical tension for rupture (38):

$$-(G_{ad} + G_{H2}) > 2\tau^*. \tag{24}$$

G_{H2} is the free energy change per unit area when the lipid in the apposed monolayers of the two membranes enters the H_{II} phase. G_{ad} is the free energy of interaction of the bilayers per unit area at the equilibrium separation between the vesicle interfaces. For PE, values of G_{ad} may be as small as -0.8 erg/cm^2 (49). G_{H2} is given by

$$G_{H2} = \frac{[\pi r_h \mu_H / a_0] - [2(r_h + l)\mu_L / \bar{a}]}{(r_h + l)} \approx \frac{\pi \Delta\mu r_h}{a_0(r_h + l)}, \tag{25}$$

where μ_H and μ_L are the chemical potentials of the H_{II} and L_α phases, respectively, and $\Delta\mu = (\mu_H - \mu_L)$. τ^* is ~3 dyne/cm for egg lecithin (24). With this value, Eq. 25 indicates that $\Delta\mu$ must be tenths of kT (T tens of degrees > T_H) in order for leakage to occur. However, the value of τ^* in H_{II}-forming systems may be much smaller than this value. The cohesion of the membranes will be lower in the regions of high curvature (i.e., junctions of the bilayers with IMI or H_{II} structures). Moreover, if the walls of the original vesicles are stressed by a trans-membrane osmotic pressure difference to a tension τ^0, then G_{H2} (Eq. 24) need only exceed the difference $2(\tau^* - \tau^0)$. In such cases, leakage may be rapid at $T \approx T_H$.

Note that apposed vesicles may not be able to leak via H_{II} formation unless the contact area A_c is big enough to contain more than one IMI. This is because the initial event in H_{II} phase formation from IMI is a two-dimensional aggregation of IMI (2): more than one IMI is required. Since n_I^0 is in the range 10^{10} to 10^{11} cm^{-2}, for $A_c \approx 10^{-11}$ to 10^{-10} cm^2, there may be on the average only one IMI between apposed vesicles at any time. In such cases, leakage and rapid H_{II} phase formation may be delayed until the vesicles fuse (via ILA formation or other mechanisms) into large structures with larger A_c. It is interesting to note that this is exactly the behavior observed in 0.2 μm diameter vesicles of mono-methylated PE (10), which should have A_c in this range. In this system, there is often a lag time between extensive aggregation of vesicles and sudden massive leakage and H_{II} formation. Some vesicle fusion is observed during this lag time. At higher temperatures, where the $L_\alpha \rightarrow H_{II}$ phase transition in bulk samples of this lipid is rapid, leakage is immediate upon aggregation. This may be a result of larger n_I^0 at higher temperatures (see Effect of Temperature on IMI and ILA Formation). Ellens et al. proposed a very similar interpretation of this data in their report (10).

Lipid Exchange Between Aggregated Vesicles

IMI make the exterior monolayers of apposed vesicles continuous for the lifetime of the IMI. Lipid molecules on the exterior monolayers of each vesicle can diffuse along the exterior surface of the IMI and onto the interface of the

apposed vesicle. We estimate the extent of lipid mixing that occurs when an IMI forms between the vesicles by calculating the distance, X_D, a lipid molecule can random-walk diffuse during the half-life of an IMI;

$$X_D \approx \left[\frac{2D}{P_{-3}}\right]^{1/2}. \quad (26)$$

P_{-3} is the rate of IMI reversion to planar bilayer patches (1, 2). If X_D is approximately the radius of the apposed vesicles, than extensive mixing of the lipid in the exterior monlayers occurs when a single IMI forms. Since D is $\sim 10^{-7}$ cm^2/s and P_{-3} for PE systems is in the range 10^3 s^{-1} (1, 2), a single IMI can extensively mix the outer monolayers of vesicles ≈ 0.1 μm in diameter.

The rate of lipid exchange is controlled by the initial rate of IMI formation between apposed vesicles. This is the product of A_c and the IMI formation rate per unit area of apposed bilayers, N_3, which is in the range 10^{11} to 10^{15} IMI cm^{-2} s^{-1} (1, 2). Since A_c is $\sim 10^{-11}$ cm^2 for 0.1 μm-diameter vesicles, IMI should form and start lipid exchange within one second or less after vesicle aggregation.

Effect of Temperature on IMI and ILA Formation

It is possible to make semi-quantitative predictions about the temperature dependence of the the membrane-membrane interactions mediated by IMI and ILA. However, $L_\alpha \leftrightarrow H_{II}$ transitions are often broad and hysteretic, and it may be hard to experimentally establish an accurate T_H for a given system. Therefore, the temperature effects predicted in this paper may occur over larger temperature ranges in real systems. Impurities (S. Gruner and G. Kirk, personal communication) and the ionic strength of the aqueous medium (39) can also affect T_H. When charged lipid impurities are present, the ionic strength of the medium can alter the rate of IMI production between vesicles by slowing the aggregation and close apposition rate. The predictions made below are valid for the zero-charge or high ionic-strength limit.

IMI are intermediates in the $L_\alpha \rightarrow H_{II}$ phase transition, and form only in the vicinity of the transition temperature, T_H. n_I^0 will change rapidly in temperature interval around T_H. We can estimate n_I^0 at different temperatures ($n_I^0[T]$) as follows. n_I^0 at T_H is given by (2)

$$n_I^0 = \frac{1}{A\left[1 + \left(\frac{P_r}{P_a}\right)\exp\left\{\frac{G^\ddagger - G_-^\ddagger}{kT}\right\}\right]}. \quad (27)$$

P_r and P_a are variables irrelevant to this discussion: it is merely important to remember that the ratio P_r/P_a is roughly constant as a function of temperature around T_H and is usually much greater than unity (2). $G^\ddagger$ and $G_-^\ddagger$ are the activation energies for IMI formation from apposed bilayers and IMI reversion to apposed bilayers, respectively. At $T = T_H$, $G^\ddagger$ is estimated to be of the order of 10 kT, and is approximately equal to $G_-^\ddagger$ (2). The difference $G^\ddagger - G_-^\ddagger$ can change as a function of temperature, changing n_I^0 (Eq. 27).

Let n_b be the number of lipid molecules composing an IMI. $G^\ddagger$ is defined as the difference in free energy of the transient activated complex of n_b lipid molecules from which an IMI forms and n_b lipid molecules in the L_α phase at $T = T_H$. $G_-^\ddagger$ is the difference between the energies of the activated complex and the IMI at $T = T_H$. Therefore the difference $G^\ddagger - G_-^\ddagger$ at temperatures around T_H is the difference in free energy of the n_b lipid molecules of the IMI and n_b molecules in the L_α phase at that temperature. This difference may have some small positive value at T_H, and will change as the relative stability of the IMI and the L_α phase changes. We do not know the temperature dependence of this difference. However, the chemical potential of the lipid in an IMI is probably similar to that of H_{II} phase lipid (1, 2), and should have a similar temperature dependence. As an approximation, we assume that the chemical potential difference between IMI and the L_α phase has the same temperature dependence as the chemical potential difference between the H_{II} and L_α phases, $\Delta\mu$.

With this approximation, at temperatures near T_H, $G^\ddagger - G_-^\ddagger$ is given by

$$G^\ddagger - G_-^\ddagger \approx n_b\Delta\mu = n_bH_H[1 - T/T_H] \quad (\text{for small } |T - T_H|), \quad (28)$$

where we have expressed $\Delta\mu$ in terms of the enthalpy of the $L_\alpha \rightarrow H_{II}$ transition, H_H. This approximation for $\Delta\mu$ is only valid for small temperature intervals around T_H (plus or minus $\sim$10°K), because H_H should change significantly over larger temperature ranges. n_b is given by (2)

$$n_b = \frac{4\pi^2(r_0 + l)r_0 - 4\pi r_0^2}{(\bar{a}a_0)^{1/2}} + \frac{4\pi r_0^2}{a_0}. \quad (29)$$

An approximation to the ratio of $n_I^0(T)$ at a temperature T near T_H to n_I^0 at T_H is thus given by (Eqs. 27 and 28; $P_r/P_a >> 1$)

$$\frac{n_I^0(T)}{n_I^0(T_H)} \approx \exp\{-n_b\Delta\mu/kT\} \quad (\text{for small } |T - T_H|). \quad (30)$$

For egg PE, H_H is ~ 0.5 kT (39), n_b is $\sim$300 (1, 2), and n_b $\Delta\mu$ increases by ~ 0.5 kT per degree K of temperature decrease below T_H. Thus, the steady-state number of IMI per unit area of vesicle-vesicle interface should be $e^{-0.5}$, $e^{-2.5}$, and e^{-5} (0.6, 0.08, and 0.007) of the value at $T = T_H$ when the temperature is 1, 5, and 10°K below T_H, respectively (Eq. 30). IMI are formed in correspondingly larger numbers, and $L_\alpha \rightarrow H_{II}$ transitions are more rapid (2), when bilayers are apposed at temperatures greater than the equilibrium T_H.

Since IMI form in exponentially decreasing numbers with decreasing temperature, IMI-mediated lipid exchange between apposed vesicles must become rare more than 5 or 10°K below T_H. At $T_H - 10°K$, $n_I^0(T)$ will be 10^8–10^9 IMI/cm^2 ($n_I^0(T_H) \approx 10^{10}$–$10^{11}$/cm^2; 2). On the average, at any given time an IMI should exist between only a small fraction of aggregated pairs of vesicles with $A_c \approx 10^{-11}$ cm^2. We cannot estimate the IMI formation and reversion rates separately as a function of temperature, since this would require knowledge of the temperature dependence of the chemical potentials of the L_α and H_{II} phases themselves. Therefore we cannot estimate the temperature dependence of the rate of IMI-mediated outer monolayer lipid mixing between vesicles. However, $G^\ddagger$ is only ~10 kT at T_H for egg PE, and since $\Delta\mu$ changes slowly with temperature, the L_α phase chemical potential may also be a slowly changing function of temperature. If this is true, the IMI formation rate could be large at temperatures as much as 10°K below T_H (the IMI formation rate at T_H is estimated to be 10^{11}–10^{15} IMI/cm^2/s; 2). The extent of vesicle outer monolayer mixing achieved by formation of a single IMI should decrease with temperature. As IMI become more and more unstable, the IMI reversion rate, P_3, should increase, which should decrease X_D (Eq. 26).

Temperature can affect the probability that two aggregated vesicles will fuse via ILA formation in two ways. This probability (P_f, Eq. 22) is the product of the number of IMI that form in the contact area ($A_c n_I^0$), P_{ILA}, and the time interval in which ILA can form. This time interval is very long when vesicles are apposed below T_H: IMI are not consumed via H_{II} formation at these temperatures, so that IMI and ILA can form as long as the vesicles remain apposed. For vesicles of dipalmitoyl- and dimyristoyl-PE, vesicle aggregates seem to be stable for hours (41). However, when the temperature is greater than or equal to T_H, the interval in which IMI and ILA can form is the $L_\alpha \rightarrow H_{II}$ phase transition time, which can be seconds or less (2, 14, 15). This several order-of-magnitude change in the interval during which ILA can form increases P_f at lower temperatures.

In contrast, n_I^0 decreases rapidly with decreasing temperature below T_H (Eq. 30). The temperature dependences of n_I^0 and the time interval for ILA formation are of opposite sign and similar magnitude, so it is not possible to make accurate estimates of the probability of fusion via ILA below T_H. It is possible that fusion via ILA will be maximal and significant only at temperatures ~2–5°K smaller than T_H, because n_I^0 will be close to the value at T_H in this range, but the H_{II} phase cannot form, so that many ILA can form (Eq. 21). The rate of fusion via ILA should decrease rapidly at $T \geq T_H$: the time interval for ILA formation decreases precipitously at T_H, and n_I^0 increases rapidly above T_H (Eq. 30), so $k_I n_I^0$ becomes much larger than P_{ILA} (Eq. 1).

DISCUSSION

All the phenomena discussed in this paper are a consequence of proximity to the $L_\alpha \rightarrow H_{II}$ phase transition. My purpose is to predict the sort and rate of membrane-membrane interaction phenomena that result from intermediates in the transition. However, membrane fusion, vesicle leakage, and lipid exchange can also occur via other mechanisms. Lipid exchange can occur slowly via single lipid molecules through the aqueous phase (e.g., 42). Vesicle leakage and fusion can occur via cation-mediated mechanisms in some systems (e.g., 35, 43). I hope to clarify the role of nonbilayer structures in membrane-membrane interactions by identifying the types and rates of interactions ascribable to them.

The analysis in this work permits four conclusions. First, IMI formation between aggregated lipid vesicles should be rapid (within 1 s or less after aggregation) at temperatures at or above T_H. Formation of a single IMI leads to extensive mixing of the lipids in the outer monolayers of the vesicles, since the lifetime of IMI (millisecond range; 1, 2) is substantial compared with the time it takes lipid molecules to diffuse a distance on the order of 0.1 μm.

Second, IMI may form in significant numbers even when the temperature is five or ten degrees below T_H, and lead to this outer monolayer mixing. The expression for the steady-state number of IMI (Eq. 30) is only an order-of-magnitude estimate, because we do not know the exact temperature dependence of the chemical potentials of IMI and the equilibrium phases. However, this method shows that membrane-membrane interactions may occur via $L_\alpha \rightarrow H_{II}$ phase transition intermediates even when the L_α phase is the equilibrium phase, although only at temperatures close to T_H.

Third, after vesicles aggregate at temperature greater or equal to T_H, the IMI that form between them will coalesce into the H_{II} phase in the same manner as in bulk multilamellar samples (2). The chemical potential gradient driving the transition drives the apposition of as much of the vesicles' surfaces as possible. This produces a tension in the vesicle walls that eventually is sufficient to rupture them. Naturally, this process can only occur at temperatures greater than T_H. The onset temperature for leakage should be slightly above T_H, but we cannot accurately predict it with Eqs. 24 and 25 because we lack accurate measurements of τ^*. It is possible that τ^* is much lower for membranes incorporating high-curvature defects like IMI, and that leakage of apposed vesicles should occur as soon as several such defects form (i.e., starting at temperatures just below T_H).

Fourth, it has previously been suggested that membrane fusion can occur via IMI-like structures ("lipidic particles", e.g., references 3, 4). These structures are thought to occur in all $L_\alpha \rightarrow H_{II}$ phase transitions (1, 2). On this basis , one would expect fusion to be rapid in vesicle dispersions of all lipid systems that can adopt the H_{II} phase

when the system is near the $L_\alpha \rightarrow H_{II}$ transition. This is not what is observed (5–10). The analysis in this paper shows that fusion only occurs when IMI form ILA, and that this should occur at observable rates only in a subset of systems with $L_\alpha \rightarrow H_{II}$ transitions. The rate of the ILA formation process is extremely sensitive to the structural parameters of the equilibrium phases (e.g., to the head group area ratio $\bar{a}/a_0$; Fig. 3), and is significant only for systems with small values of this ratio. The critical $\bar{a}/a_0$ ratio for significant fusion rates (i.e., $P_{ILA} \approx 1$, Eq. 1) cannot be accurately predicted, but it is likely to be in the range of 1.2. In pure, unsaturated acyl-chain PE systems, this ratio is observed to be much larger (~1.8 for egg PE; 16, 17). Hence, fusion via ILA formation should be rare in such systems, which should include most PEs of biological interest. Fusion may occur in some systems with large $\bar{a}/a_0$ ratios if the bilayer lateral compressibility is fairly large (e.g., 0.02 dyn/cm or larger, compared to the observed values of 0.007–0.01 dyn/cm; 24–26). ILA formation rates in systems with large $\bar{a}/a_0$ ratios should be maximal at temperatures a few degrees below T_H: to whatever extent fusion via ILA occurs in such systems, it should be most observable in that temperature range.

Ellens, Bentz, Szoka and co-workers (5–8) have recently studied the interactions of large uni- and oligo-lamellar vesicles composed of egg PE and small mole fractions of cholesteryl hemisuccinate (CHEMS). They have also studied vesicle dispersions of three different pure PEs (9). Thermotropic $L_\alpha \rightarrow H_{II}$ phase transitions can occur in such systems when the ambient pH is low and CHEMS and PE are in the protonated, uncharged form. The temperature-dependent interactions of vesicles around T_H at low pH reported by these authors are those predicted by the present model. Vesicles in these systems leak their aqueous contents to the surrounding medium in an aggregation-dependent manner (5, 8, 9). Lipid mixing occurs both above and below T_H (7). However, the initial rate of lipid mixing after vesicle aggregation reflects the kinetics of intermediate formation between the vesicles. This initial rate of lipid mixing is small at low temperatures and increases rapidly with increasing temperature near T_H, reaching a plateau a few degrees below T_H (7, 9). The initial rate of aggregation-induced leakage also increases rapidly with temperature in the immediate vicinity of T_H. Fusion is not observed at all in CHEMS-PE at low pH (7, 8). At low pH, small fusion rates are observed in the pure PE systems (9) when the temperature is below T_H, but these rates are maximal a few degrees below T_H and fall to very small values at temperatures above T_H.

These are exactly the attributes predicted in this work for lipids with rapid thermotropic transitions like PE: P_f is very small (fusion unobservable for $T \geq T_H$); leakage occurs after vesicle aggregation via H_{II} formation at $T \geq T_H$; and lipid mixing (via IMI formation) begins at temperatures slightly below T_H. It is possible that the liposome fusion observed a few degrees below T_H in pure PE systems (9) is ILA-mediated. Since IMI that form at these temperatures cannot be consumed by H_{II} phase formation, the rate of ILA formation from IMI may be significant even if the value of $\bar{a}/a_0$ is not optimal for ILA formation (Eq. 1). ILA production would be slow compared to H_{II} phase production at $T \geq T_H$, and fusion would stop, as is observed (9).

The same authors, in a recent study of mono-methylated dioleoyl-PE (10), observed rapid initial lipid mixing and leakage rates in a temperature range in which bulk samples had a rapid $L_\alpha \rightarrow H_{II}$ transition, but observed increased rates of membrane fusion and reduced leakage rates at lower temperatures, where bulk samples adopted isotropic or cubic phases (18). These observations are compatible with the postulate that ILA produce both membrane fusion and cubic ("isotropic") phase formation (D. P. Siegel, manuscript submitted for publication; and below), while IMI, which are most numerous when $L_\alpha \rightarrow H_{II}$ transitions are rapid (2), mediate only lipid exchange and vesicle leakage. Mono-methylated PE is a lipid that one would expect to have an $\bar{a}/a_0$ ratio much closer to 1.2 (i.e., $P_{ILA} \approx 1\ s^{-1}$) than to the value of ~1.8 observed for egg PE ($P_{ILA} \approx 0$). PEs and PCs of similar unsaturated acyl chain distributions have similar areas per head group in the L_α phase (17). Mono-methylated PE, having a head group structure intermediate between PE and PC (mono- vs. tri-methylated as in PC) is likely to have nearly the same value of $\bar{a}$ in the L_α phase as PE and PC. The slightly larger mono-methylated PE head group will be more difficult to pack into a highly curved H_{II} phase lipid-water interface, resulting in a larger value of a_0 and a smaller ratio $\bar{a}/a_0$. Thus, the observations of isotropic phase structures in mono- vs. unmethylated DOPE (18) and of fusion in such systems (10) and not in DOPE (9) are all consistent both with the concept of ILA-mediated fusion and with the increasing incidence of ILA as a function of decreasing $\bar{a}/a_0$ predicted in this work.

The fact that multilamellar samples of mono-methylated DOPE form isotropic phases at low temperatures but H_{II} phases at higher temperatures (10, 18) may be due to an increase in n_I^0 with increasing temperature (Eq. 30). This would increase the rate of H_{II} phase formation relative to P_{ILA} at high temperatures (Eq. 1). Also, isotropic phases may not form at high temperatures because P_{ILA} may be smaller due to an increase in $\bar{a}/a_0$ (Fig. 3; Eq. 7) with increasing temperature. In a similar mixed PE-PC system (20), the radius of curvature of the H_{II} phase has been observed to decrease with increasing temperature, which is consistent with an increase in $\bar{a}/a_0$. In this work, T_H is defined as the temperature at which the H_{II} phase first becomes the stable phase at equilibrium. In mono-methylated DOPE, T_H is probably the temperature at which the isotropic phase is first observed. At such temperatures, H_{II} is the equilibrium phase, but the $L_\alpha \rightarrow H_{II}$ phase transition is sluggish, and the intermediates in it (IMI) become trapped via ILA formation. ILA are metastable structures

that cannot assemble into the H_{II} phase (D. P. Siegel, manuscript submitted for publication).

Ellens et al. (9) also studied interactions of PE liposomes as a function of temperature near $L_\alpha \rightarrow H_{II}$ transitions induced by Ca^{2+} addition at pH 9.5, where PE is anionic. It is not clear if such transitions should be classified as ionotropic. The resulting H_{II} phase has the same T_H as the transition observed at low pH in the absence of Ca^{2+}. Also, high concentrations of Ca^{2+} are required (20 mM) to form the H_{II} phase at pH 9.5. These facts imply that stable Ca^{2+}-PE complexes of defined stoichiometry may not form. Ca^{2+} may simply reside in the electrical double layer, reducing the net electrostatic repulsion between anionic PE head groups, and allowing them to pack closely together to form the high-curvature lipid-water interface of the H_{II} phase. The temperature-dependent liposome interactions in Ca^{2+}-PE are the same as in PE at low pH, and are as predicted here for thermotropic systems with rapid $L_\alpha \rightarrow H_{II}$ transitions. The Ca^{2+}- and Mg^{2+}-induced interactions in CHEMS-PE (6, 8) are as predicted here for ionotropic systems (below). In CHEMS-PE, Ca^{2+} induces an H_{II} phase with a higher T_H than the low-pH H_{II} phase, and only small concentrations of Ca^{2+} are required. This is what one would expect for an ionotropic transition (i.e., stable anionic lipid-cation complexes of defined stoichiometry).

Therefore, the present model of membrane-membrane interactions provides a consistent and unified description of membrane-membrane interactions in these systems near the $L_\alpha \rightarrow H_{II}$ phase transition. The authors of reference 10 arrived at a similar interpretation of their findings. Elsewhere (D. P. Siegel, manuscript submitted for publication), I will describe how ILA can assemble into arrays with the observed attributes of the inverted cubic and amorphous phases described by others (18, 20, 21).

Lipids with $L_\alpha \rightarrow H_{II}$ Transitions Driven by Cation-Binding

In some lipid systems, the $L_\alpha \rightarrow H_{II}$ phase transition is driven by the binding of cations to anionic lipid molecules. Cardiolipin (11, 12) and phosphatidic acid (44, 45) adopt the H_{II} phase in the presence of divalent cations or acid (47). The kinetics of such transitions and IMI/ILA formation cannot be quantitatively described by the theory in reference 2. $\Delta\mu$ is a sensitive function of the interfacial curvature and local cation concentration, and the free energy of intermediates of different curvature will be quite different. Thus the free energies of activation for interconversion of structures will be different than calculated here, and their populations will be in different ratios.

It is likely that for given $\tilde{n}_c$ values, P_f will be larger for systems with transitions driven by cation binding than for systems with thermotropic transitions. The activation energies for reversion and coalescence of IMI into H_{II}-like structures will be large, since substantial changes in interfacial curvature (and dissociation of many lipid-cation complexes) are involved. In contrast, formation of ILA from IMI involves almost no change in the area of IMI interface having curvature resembling the H_{II} phase. The activation energy for ILA formation may thus be smaller than the activation energy for reversion to planar bilayers, and ILA may form at a greater rate than in thermotropic systems. Moreover, in the presence of cation concentrations much above the transition threshold value, ILA will be more stable than patches of planar bilayer: the lipids on the exterior monolayer will have H_{II} like curvature, and $\Delta\mu$ relative to the bilayer should be of order kT in the presence of excess Ca^{2+} (11). Hence, ILA formation (and ILA-mediated fusion) are more probable in systems with transitions driven by cation-binding.

In their study (47) of cardiolipin/phosphatidylcholine vesicle fusion, Wilschut et al. reported that, on exposure to Ca^{2+}, fusion (mixing of aqueous contents of vesicles) became observable at a fairly well-defined threshold Ca^{2+} concentration. The initial rate of fusion increased rapidly at concentrations above this threshold. The leakage rate also increased with increasing Ca^{2+} concentrations above this threshold, until it was almost as fast as fusion. This is the behavior expected in a system in which the rate of IMI coalescence into H_{II} precursors is smaller than P_{ILA}. As $[Ca^{2+}]$ increases past the threshold value, $\Delta\mu$ increases, and the ILA formation (fusion) rate increases. The leakage rate is slow at near-threshold $[Ca^{2+}]$ since IMI coalescence (H_{II} phase formation) is slow. The rate of leakage increases at higher $[Ca^{2+}]$ because n_I^0, the IMI coalescence rate (Eq. 1), and G_{H2} (Eq. 25) all increase with $[Ca^{2+}]$. Thus, the $[Ca^{2+}]$ dependences of the interaction rates in this system are compatible with an IMI- and ILA-based mechanism. However, other mechanisms cannot be ruled out, and ILA-mediated fusion has not been unambiguously demonstrated.

Possible Biological Relevance

As described in Part I (2), many biomembranes and membrane lipid extracts can adopt the H_{II} phase or form IMI/ILA-like morphology if slightly dehydrated. Moreover, small changes in the composition of these biomembranes can destabilize them with respect to H_{II} phase formation (for reviews, see references 19, 48). It is possible that cells could control the susceptibility of specific areas of their membranes to membrane fusion (e.g., as in exocytosis) via ILA by subtle modulation of the amounts of lipids that stabilize the H_{II} phase at physiological temperatures. This and other possible roles of IMI and ILA structures in biomembrane behavior will be discussed elsewhere (48).

The author is extremely grateful to J. Bentz, H. Ellens, and F. C. Szoka for many helpful discussions of PE system behavior, and to D. F. Hager and J. R. Hansen for much helpful editing advice and encouragement.

Received for publication 3 April 1985 and in final form 17 January 1986.

REFERENCES

1. Siegel, D. P. 1984. Inverted micellar structures in bilayer membranes. *Biophys. J.* 45:399–420.
2. Siegel, D. P. Inverted micellar intermediates and the transitions between lamellar, cubic, and inverted hexagonal lipid phases. I. Mechanism of the $L_\alpha \leftrightarrow H_{II}$ phase transitions. *Biophys. J.* 49:1155–1170.
3. Cullis, P. R., B. de Kruijff, M. J. Hope, A. J. Verkleij, R. Nayar, S. B. Farren, C. Tilcock, T. D. Madden, and M. B. Bally. 1983. Structural properties of lipids and their functional roles in biological membranes. *In* Membrane Fluidity in Biology. Vol. 1. Academic Press, Inc., NY. 39–81.
4. Verkleij, A. J., C. Mombers, W. J. Gerritsen, L. Leunissen-Bijvelt, and P. R. Cullis. 1979. Fusion of phospholipid vesicles in association with the appearance of lipidic particles as visualized by freeze fracturing. *Biochim. Biophys. Acta.* 555:358–361.
5. Ellens, H., J. Bentz, and F. C. Szoka. 1984. pH-induced destabilization of phosphatidylethanolamine-containing liposomes: role of bilayer contact. *Biochemistry.* 23:1532–1538.
6. Lai, M.-Z., W. J. Vail, and F. C. Szoka. 1985. Acid and calcium induced structural changes in phosphatidylethanolamine membranes stabilized by cholesterylhemisuccinate. *Biochemistry.* 24:1654–1661.
7. Bentz, J., H. Ellens, M.-Z. Lai, and F. C. Szoka. 1985. On the correlation between H_{II} phase and contact-induced destabilization of membranes. *Proc. Nat'l. Acad. Sci. USA.* 82:5742–5745.
8. Ellens, H., J. Bentz, and F. C. Szoka. 1985. H^+ and Ca^{2+}-induced fusion and destabilization of liposomes. *Biochemistry.* 24:3099–3106.
9. Ellens, H., J. Bentz, and F. C. Szoka. 1985. Destabilization of phosphatidylethanolamine liposomes at the hexagonal phase transition temperature. *Biochemistry.* 25:285–294.
10. Ellens, H., J. Bentz, and F. K. Szoka. 1986. Fusion of phosphatidylethanolamine containing liposomes and the mechanism of the L_α-H_{II} phase transition. *Biochemistry.* In press.
11. De Kruijff, B., A. J. Verkleij, J. Leunissen-Bijvelt, C. J. A. van Echteld, J. Hille, and H. Rijnbout. 1982. Further aspects of the Ca^{2+}-dependent polymorphism of bovine heart cardiolipin. *Biochim. Biophys. Acta.* 693:1–12.
12. Rand, R. P., and S. Sengupta. 1972. Cardiolipin forms hexagonal structures with divalent cations. *Biochim. Biophys. Acta.* 255:484–492.
13. Hui, S. W., T. P. Stewart, P. L. Yeagle, and A. D. Albert. 1981. Bilayer to non-bilayer transition in mixtures of phosphatidylethanolamine and phosphatidylcholine: implications for membrane properties. *Arch. Biochem. Biophys.* 207:227–240.
14. Ranck, J. L., L. Letellier, E. Schechter, B. Krop, P. Pernot, and A. Tardieu. 1984. X-ray analysis of the kinetics of *E. coli* lipid and membrane structural transitions. *Biochemistry.* 23:4955–4961.
15. Caffrey, M. 1985. Kinetics and mechanism of the lamellar gel/lamellar liquid crystal and lamellar/inverted hexagonal phase transition in phosphatidylethannolamine: a real-time x-ray diffraction study using synchrotron radiation. *Biochemistry.* 24:4826–4844.
16. Reiss-Husson, F. 1967. Structure des phases liquide-crystalline de differents phopholipides, monoglycerides, sphingolipides, anhydres ou en presence d'eau. *J. Möl. Biol.* 25:363–382.
17. Lis, L., M. McAlister, N. Fuller, R. P. Rand, and V. A. Parsegian. 1982. Interactions between neutral phospholipid membranes. *Biophys. J.* 37:657–666.
18. Gagné, J., L. Stamatatos, T. Diacovo, S. W. Hui, P. L. Yeagle, and J. R. Silvius. 1985. Physical properties of bilayer membranes containing N-methylated phosphatidylethanolamines. *Biochemistry.* 24:4400–4408.
19. Verkleij, A. J. 1984. Lipidic intramembranous particles. *Biochim. Biophys. Acta.* 779:43–63.
20. Boni, L. T., and S. W. Hui. 1983. Polymorphic phase behavior of dilinoleoylphosphatidylethanolamine and palmitoyloleoylphosphatidylcholine mixtures: structural changes between hexagonal, cubic, and bilayer phases. *Biochim. Biophys. Acta.* 731:177–285.
21. Hui, S. W., T. P. Stewart, and L. T. Boni. 1983. The nature of lipidic particles and their roles in polymorphic transitions. *Chem. Phys. Lipids.* 33:113–126.
22. Vaz, W. L. C., M. Criado, V. M. C. Madeira, G. Schoellmann, and T. M. Jovin. 1982. Size dependence of the translational diffusion of large integral membrane proteins in liquid-crystalline phase lipid bilayers: a study using fluorescence recovery after photobleaching. *Biochemistry.* 21:5608–5612.
23. Peters, R., and R. J. Cherry. 1982. Lateral and rotational diffusion of bacteriorhodopsin in lipid bilayers: experimental test of the Saffman-Delbruck equations. *Proc. Natl. Acad. Sci. USA.* 79:4317–4321.
24. Kwok, R., and E. Evans. 1981. Thermoelasticity of large lecithin bilayer vesicles. *Biophys. J.* 35:637–652.
25. Evans, E., and R. Kwok. 1982. Mechanical calorimetry of large dimyristoylphosphatidylcholine vesicles in the phase transition region. *Biochemistry.* 21:4874–4879.
26. Smaby, J. M., A. Hermetter, P. C. Schmid, F. Patlauf, and H. L. Brockman. 1983. Packing of ether and ester phospholipids in monolayers. Evidence for hydrogenbonded water at the *sn*-1 acyl group of phosphatidylcholines. *Biochemistry.* 22:5808–5813.
27. Rand, R. P., and V. A. Parsegian. 1983. Physical force considerations in model and biological membranes. *Can. J. Biochem. Cell Biol.* 62:752–759.
28. White, S. H., and G. I. King. 1985. Molecular packing and area compressibility of lipid bilayers. *Proc. Natl. Acad. Sci. USA.* 82:6532–6536.
29. Kirk, G. L., S. M. Gruner, and D. L. Stein. 1984. A thermodynamic model of the lamellar to inverse hexagonal phase transition of lipid membrane-water systems. *Biochemistry.* 23:1093–1102.
30. Sakurai, I., and Y. Kawamura. 1983. Magnetic-field-induced orientation and bending of the myelin figures of phosphatidylcholine. *Biochim. Biophys. Acta.* 735:189–192.
31. Servuss, R. M., W. Harbich, and W. Helfrich. 1976. Measurement of the curvature elastic modulus of egg lecithin bilayers. *Biochim. Biophys. Acta.* 436:900–903.
32. Schneider, M. B., J. T. Jenkins, and W. W. Webb. 1984. Thermal fluctuations of large cylindrical phospholipid vesicles. *Biophys. J.* 45:891–899.
33. Bentz, J., S. Nir, and J. Wilschut. 1983. Mass action kinetics of vesicle aggregation and fusion. *Colloids Surf.* 6:333–363.
34. Nir, S., J. Bentz, J. Wilschut, and N. Duzgunes. 1983. Aggregation and fusion of phospholipid vesicles. *Prog. Surf. Membr. Sci.* 13:1–124.
35. Bentz, J., N. Duzgunes, and S. Nir. 1983. Kinetics of divalent cation-induced fusion of phosphatidylserine vesicles: correlation between fusogenic capacities and binding affinities. *Biochemistry.* 22:3320–3330.
36. Nir, S., J. Wilschut, and J. Bentz. 1982. The rate of fusion of phospholipid vesicles and the role of bilayer curvature. *Biochim. Biophys. Acta.* 688:275–278.
37. Nir, S., N. Duzgunes, and J. Bentz. 1983. Binding of monovalent cations to phosphatidylserine and modulation of Ca^{2+}- and Mg^{2+}-induced vesicle fusion. *Biochim. Biophys. Acta.* 735:160–172.
38. Parsegian, V. A., and R. P. Rand. 1983. Membrane interactions and deformation. *Ann. NY Acad. Sci.* 416:1–12.
39. Seddon, J. M., G. Cevc, and D. Marsh. 1983. Calorimetric studies of the gel-fluid and lamellar-inverted hexagonal phase transition in dialkyl- and diacylphosphatidylethanolamines. *Biochemistry.* 22:1280–1289.
40. Hardmann, P. D. 1982. Spin-label characterization of the lamellar-to-H_{II} phase transition in egg phosphatidylethanolamine. *Eur. J. Biochem.* 124:95–101.

41. Kolber, M. A., and D. H. Haynes. 1979. Evidence for a role of phosphatidylethanolamine as a modulator of membrane-membrane contact. *J. Membr. Biol.* 48:95–114.
42. McLean, L. R., and M. C. Phillips. 1984. Kinetics of phosphatidylcholine and lysophosphatidylcholine exchange between unilamellar vesicles. *Biochemistry.* 23:4624–4630.
43. Wilschut, J., and D. Papahadjopoulos. 1979. Ca^{2+}-induced fusion of phospholipid vesicles monitored by mixing of aqueous contents. *Nature* (*Lond.*). 281:690–692.
44. Verkleij, A. J., R. De Maagd, J. Leunissen-Bijvelt, and B. de Kruijff. 1982. Divalent cations and chloropromazine can induce nonbilayer structures in phosphatidic acid-containing bilayers. *Biochim. Biophys. Acta.* 684:255–262.
45. Miner, V. W., and J. H. Prestegard. 1984. Structure of cation-phosphatidic acid complexes as determined by ^{31}P-NMR. *Biochim. Biophys. Acta.* 774:227–236.
46. Seddon, J. M., R. D. Kaye, and D. Marsh. 1983. Induction of the lamellar-inverted hexagonal phase transition in cardiolipin by protons and monovalent cations. *Biochim. Biophys. Acta.* 734:347–352.
47. Wilschut, J., M. Holsappel, and R. Jansen. 1982. Ca^{2+}-induced fusion of cardiolipin/phosphatidylcholine vesicles monitored by mixing of aqueous contents. *Biochim. Biophys. Acta.* 690:297–301.
48. Siegel, D. P., Membrane-membrane interactions via intermediates in lamellar-to-inverted hexagonal phase transitions. *In* Membrane Fusion. A. E. Sowers, editor. Plenum Publishing Corp. In press.
49. Marra, J., and J. Israelachvili. 1985. Direct measurements of forces between phosphatidylcholine and phosphatidylethanolamine bilayers in aqueous electrolyte solutions. *Biochemistry.* 24:4608–4618.